Insights into the absorption of hydrocarbon gases in phosphorus-containing ionic liquids

McCalmont, S., M. Vaz, I. C., Oorts, H., Gong, Z., Moura, L., & Costa Gomes, M. (2023). Insights into the absorption of hydrocarbon gases in phosphorus-containing ionic liquids. *Journal of Physical Chemistry B*, *127*(15), 3402-3415. https://doi.org/10.1021/acs.jpcb.2c08051

Queen's University Belfast - Research Portal:
Link to publication record in Queen's University Belfast Research Portal

Insights into the absorption of hydrocarbon gases in phosphorous-containing ionic liquids

Sam H. McCalmont,[†] Inês C.M. Vaz,[‡] Hanne Oorts,[‡] Zheng Gong,[‡] Leila Moura*,[†] and Margarida Costa Gomes*,[‡]

†*QUILL Research Centre, Queen's University Belfast, School of Chemistry and Chemical Engineering, David Keir Building, 39-123 Stranmillis Road, Belfast, BT9 5AG, Belfast, UK*

‡*Laboratoire de Chimie de l'ENS Lyon, CNRS and Université de Lyon, 46 allée d'Italie, 69364 Lyon, France*

E-mail: Margarida.Costa-Gomes@ens-lyon.fr;L.Moura@qub.ac.uk

Abstract

The solubility of ethane, ethylene, propane and propylene were measured in two phosphorous-containing ionic liquids, trihexyltetradecylphosphonium bis(2,4,4-trimethylpentyl)phosphinate, $[P_{6,6,6,14}][DiOP]$, and 1-butyl-3-methylimidazolium dimethylphosphate, $[C_4C_1Im][DMP]$, using an isochoric saturation method. The ionic liquid $[C_4C_1Im][DMP]$ absorbed between 1 and 20 molecules of gas per each 1000 ion pairs, at 313 K and 0.1 MPa, while $[P_{6,6,6,14}][DiOP]$ absorbed up to 169 molecules of propane per each 1000 ion pairs in the same conditions. $[C_4C_1Im][DMP]$ showed higher capacity to absorb olefins than paraffins, while the opposite was true for $[P_{6,6,6,14}][DiOP]$, the former being slightly more selective than the later. From the analysis of the thermodynamic properties of solvation, we concluded that in both ionic liquids and for all the studied gases, the solvation is ruled by the entropy, even if its contribution is unfavorable. These results, together with density measurements, 2D NMR studies and self-diffusion coefficients suggest that the gases' solubility is ruled mostly by non-specific interactions with the ionic liquids and that the looser ion packing in $[P_{6,6,6,14}][DiOP]$ makes it easier to accommodate the gases compared to $[C_4C_1Im][DMP]$.

Introduction

Separation processes in chemical engineering account for 10-15% of the global energy consumption. Cryogenic distillation operations for light hydrocarbon separation alone correspond roughly to 0.3% of the world energy demand, around 30 months of the UK energy demand, with corresponding greenhouse gas emissions.[1,2] This is due to the very high global demand (over 250 million tons annually and growing) of high purity (99.9%) light olefins, along with their close boiling points and small relative volatilities compared to their saturated counterparts.[3] Considerable research has been dedicated to the discovery of alternative materials and technologies that could provide sustainable and low-energy alternatives to cryogenic distillation, as these would have a major impact on emissions and pollution, while opening new routes to resources. Among the most recent alternatives studied are molecular organic frameworks (MOFs) and other porous materials,[4–9] polymers,[10] porous liquids,[11] and a variety of membrane types.[12–17] Most of these alternatives make use of transition metals such as copper or silver, due to their ability to form a complex with the unsaturated gas.[18] However, the use of said metals has certain drawbacks when it comes to their industrial scale applicability such as the irreversible reaction of the metal ions with common hydrocarbon stream contaminants. Alkynes can form explosive acetylides; sulfur compounds are able to produce insoluble metal sulfides and hydrogen; and the presence of light can lead to the reduction of the metal ions.[1] Cost, complexity of production and stability issues are other drawbacks associated with some of the explored alternatives. Furthermore, absorption is the second most technological and usage mature separation operation after distillation, which would facilitate the adoption of novel absorbents by industry.[19] A popular class of absorbent materials suggested for hydrocarbon separation are ionic liquids.[20,21]

Ionic liquids (ILs) are salts with a melting temperature below 100 °C, many being liquid at room temperature and have found a wide range of applications in industry.[22] Some of their most interesting assets are the tuning of relevant properties brought by the different combinations of anions and cations and low volatilities, which avoids the contamination of

the gas streams. In 2016, Moura *et al.* reviewed the state of the art concerning the usage of ionic liquids for hydrocarbon separations.[20] The authors observed that the ionic liquids that produce the highest solubility of ethylene are phosphorous based ionic liquids, particularly those with large hydrocarbon domains both in the cation and anion. Ethane and ethylene solubilities were found to be particularly high in the tetradecyl(trihexyl)phosphonium bis(2,4,4-trimethylpentyl)phosphinate ionic liquid, $[P_{6,6,6,14}][DiOP]$, with Henry's law constants, K_H, of 19 MPa and 36 MPa at 313 K, respectively. Liu *et al.* observed that this ionic liquid produced the lowest reported selectivity towards ethylene against ethane (0.5), due to a preferential solubility towards ethane, the opposite observed for the majority of ionic liquids tested so far.[20] The authors of the original work attributed this result to the stronger solute-solvent interactions between alkanes and the ionic liquid compared to their unsaturated counterparts.[23,24] This trend is somewhat consistent with what Moura *et al.* noted in ionic liquids containing an imidazolium-based cation with a saturated alkyl side chain and a bis(trifluorosulfonyl)imide anion, since ethane seemed preferentially solvated around the hydrocarbon moiety but furthest from the imidazolium ring. However, it was noted that in this case, it is the favorable entropy of solvation that is responsible for the selectivity of the absorption of the two gases, with ethylene being the more soluble.[25] The use of phosphonium based ionic liquids have also been used for other hydrocarbon solubilities and separations, for example acetylene and ethylene separations, including different length chains of alkyl groups on the phosphorus cation.[26–28]

The ionic liquids that are known to have the highest selectivities towards ethylene over ethane have the inclusion of nitrile groups, 1-(3-cyanopropyl)-3-methylimidazolium dicyanamide, $[C_3C_1CNIm][DCA]$ and 1,3-(3-cyanopropyl)imidazolium bis(trifluoromethylsulfonyl)-imide, $[(C_3CN)_2Im][NTf_2]$ with selectivities of 2.1 and 2.0, respectively.[29,30] However, these same ionic liquids also have some of the lowest observed absorption capacity for both ethane and ethylene, with K_H of 757 MPa and 357 MPa in the first ionic liquid and K_H being 19 MPa and 36 MPa in the second at 313 K, respectively. In both cases the authors concluded

that the difference in solubility of the two gases in each IL is due to non-specific interactions.

Moura *et al.* observed that the general tendencies for ethane, ethylene, propane and propylene absorption in a wide variety of ionic liquids are similar. The increasing size of the non-polar domains of the cation or anion of the ionic liquid is the dominant factor leading to the increase of gas solubility, which suggests that the solubility of these gases in the group of ionic liquids studied is consistently ruled by nonspecific interactions. The solubility order in terms of cation type is: $[P_{nmpq}]^+ > [C_nPyr]^+ > [C_nC_mPyrr]^+ > [C_nC_mIm]^+$, meaning, in order, phosphonium, pyridinium, pyrrolidinium and imidazolium cations.[20] In comparison, the solubility dependency in terms of the nature of the anion is much smaller, for the same gases. Again, some phosphate/phosphinate based ionic liquids stand out for their particularly high capacity to absorb low molecular weight hydrocarbons.[20,24]

Liu *et al.* focused on propane and propylene separation utilising 1-hexyl-3-methylimidazolium trifluoromethanesulfonate and hexafluorophosphate.[31] The result were selectivities towards propylene from propane of 1.1 and 1.9, respectively. Consistent with previous findings, the authors agreed that ionic liquids with high molar volume should have good performance for olefin and paraffin separation, as the cation and anion dictates the free volume in the salt and so directly influence the solubility/selectivity of the gases. While investigating ionic liquids for the separation of a higher paraffin, n-butane, from water, Makino *et al.* observed the same tendencies. Ionic liquids with longer alkyl chains in the cation and anion lead to an increase in non-specific/van der Waals molecular interactions with the gas and to an increase in the free volume, and consequently an increase in gas solubility.[32]

Xu *et al.* utilise deep eutectic solvents, DES, for the separation of ethane and ethylene, a group of materials considered analogous to ionic liquids.[33] Eutectic mixtures are formed when two or more components produce a homogeneous liquid mixture for which the melting point is reduced when compared to the melting points of the isolated components. Strictly speaking, the designation DES is applied for mixtures for which the eutectic temperature is substantially smaller than the correspondent ideal mixture. However, in the research

community it is generally accepted that many of these liquid mixtures, including outside of the eutectic compositions can also be designated DES.[34] In this study, Xu and coworkers used different mixtures of tetrabutylammonium chloride and n-decanoic acid, obtaining tunable selectivities towards ethylene to ethane between 0.8 and 1.3. The authors attribute the higher absorption of ethylene to a balance between stronger interactions of this gas with the DES components and a negative effect of the gas absorption on the free volume of the DES.The mixture producing selectivity of 1.3 was subjected to 10 regeneration cycles, and the selectivity remained constant throughout.

Despite the known obstacles to implementation in an industrial setting, materials containing silver and copper salts are still a popular research topic for hydrocarbon separation, including in ILs and DES. Recently, a series of double-salted ionic liquids derived facilitated transport membranes have been developed by Xu, Jiang and coworkers, which incorporate the use of silver nitrate as an ethylene carrier.[35] The ionic liquid mixtures consisted of different compositions of propylamine nitrate, [PA][NO$_3$], butylamine nitrate, [BA][NO$_3$], 1-ethylimidazolium nitrate, [C$_2$Im][NO$_3$], pyrrolidium nitrate, [Pyr][NO$_3$], ethanolamine nitrate, [EoA][NO$_3$], and aminopropanol nitrate, [PoA][NO$_3$]. The mixtures being tested included [PA][EoA][NO$_3$], [PA][EoA][NO$_3$], [PA][EoA][NO$_3$], [C$_2$Im][EoA][NO$_3$], [C$_2$Im][PoA][NO$_3$], and [C$_2$Im][PoA][NO$_3$] and [Pyr][EoA][NO$_3$]. The ethylene permeability of the membranes (the movement of gas through the membrane) was higher than that of ethane, which is expected due to the use of the silver salt. The durability of the [PA][PoA][NO$_3$] membrane was tested for at least 150 hours, with the selectivity remaining above 60 for ethylene to ethane and satisfactory carrier stability under light and hydrogen atmosphere for the duration of the stability study. Interestingly, the mixing of ionic liquids increased the selectivity towards ethylene compared to one single ionic liquid, even when both contained silver salts.

The separation of propylene and propane were tested in 1-hexyl-3-methylimidazolium bis(trifluoromethylsulfonyl)imide, [C$_6$C$_1$Im][NTf$_2$] and 1-hexyl-2,3-dimethylimidazolium

bis(trifluoromethylsulfonyl)imide, $[C_6C_1C_1Im][NTf_2]$, supported ionic liquid membranes, with incorporated silver salt.[36] Without the use of silver, a selectivity of propylene over propane of 2 was observed, whereas it increased to up to 8 for membranes containing $[C_6C_1C_1Im][NTf_2]$ and 1 M of silver ions. The authors were intrigued that the presence of the ionic liquid seemed to enhance the silver salt stability in the presence of hydrogen gas compared to silver salt stability in polymer membranes. Park *et al.* investigated this effect and found that anions such as bis(trifluoromethylsulfonyl)imide and trifluoromethane-sulfonate aggregate around silver ions, protecting them against reduction by hydrogen, when compared to nitrate anions.[37] The supported ionic liquid membrane containing 1.7 M Ag^+ and $[C_6C_1Im][NTf_2]$ maintained a selectivity of 8.2 ethylene to ethane for the duration of a 7 day process.

Liang *et al.* incorporated a silver ion containing ionic liquid onto a covalent organic framework (COF) membrane.[38] The COF-IL membrane was exposed to a mixture of ethylene/ethane, and depending on the silver ionic liquid loading ranged from ethylene to ethane selectivity ranging from 10 to 112. A 60% loading of the silver based ionic liquid was the best performing system, as any loading above this value seemed to a decrease in pore channel value, decreasing the ability of ethylene to enter and a decrease in selectivity. The top-performing membrane was exposed to a gas mixture containing hydrogen and the selectivity was kept at 112 for a test period of 168 hours. In the same conditions the IL membrane with no silver ions included presented selectivity below 2.5.

The use of silver has also been tested in DES, using it as a carrier and stabiliser for the silver salt and incorporated into membranes.[15] Dou *et al.* produce mixtures of dimethylam-monium nitrate or triethylammonium nitrate and ethylene glycol or triethylene glycol as DES components, while silver nitrate was applied as the silver carrier. A max selectivity of ethylene to ethane of 100 was observed. Although stable even in the presence of hydrogen for 6 months, the authors expect silver poisoning from the presence of sulfur compounds in the industrial gas streams. Dou *et al.* designed supported ionic liquids membranes with

high carrier efficiency via strong hydrogen-bond basicity that included a silver carrier. Their top-performer was 1- ethyl-3-methylimidazolium diethylphosphate, $[C_4C_1Im][DEP]$ achieved a ethylene to ethane selectivity of 39.6 with a $Ag[BF_4]$ loading of 2 M for over 160h. However the membrane was not tested in the presence of common gas stream contaminants or light.[14] Researchers from the same group have reported the first boron nitride membrane tested for gas separation. This membrane presents tailored nanosized channels and a distinct nanoconfinement effect, shedding light on the development of advanced molecular separation membranes. The nanochannels are decorated with a silver salt containing IL, 1-ethylimidazolium nitrate, contributing to the high ethylene permeance and selectivity of up to 128, and 180 h stability, both higher than the reported state of the art membranes. However, the authors do not comment on the stability of the membranes to common has stream contaminants of the presence of light.[39]

In this work, the absorption of ethane, ethylene, propane and propylene was measured in phosphorous-containing ionic liquids, trihexyltetradecylphosphonium bis(2,4,4-trimethyl-pentyl)phosphinate $[P_{6,6,6,14}][DiOP]$, in figure 1 and 1-butyl-3-methylimidazolium dimethyl-phosphate $[C_4C_1Im][DMP]$ in figure 2. Our goal is to further the understanding of the role and impact of the presence of phosphorus in the anion and cation of the IL in the differential absorption of ethane/ethylene and propane/propylene gas pairs.

As the solubility of these gases in $[C_4C_1Im][DMP]$ and $[P_{6,6,6,14}][DiOP]$ was precisely measured at different temperatures, the thermodynamic properties of solvation could be derived, providing insights into the observed trends. The ideal selectivity of the gas absorption was also calculated allowing for the evaluation of the potential of the use of these ionic liquids to separate gaseous alkane/alkene mixtures. Nuclear magnetic resonance (NMR) studies complement the gas solubility measurements in an effort to detect the effect and possible interactions of the gases in the ionic liquids. The 1D and 2D NMR spectroscopy results enable the determination of the self-diffusion coefficients of the ionic liquids pure and in the gas solutions.

Methods

Materials

Synthesis of [P$_{6,6,6,14}$][DiOP]
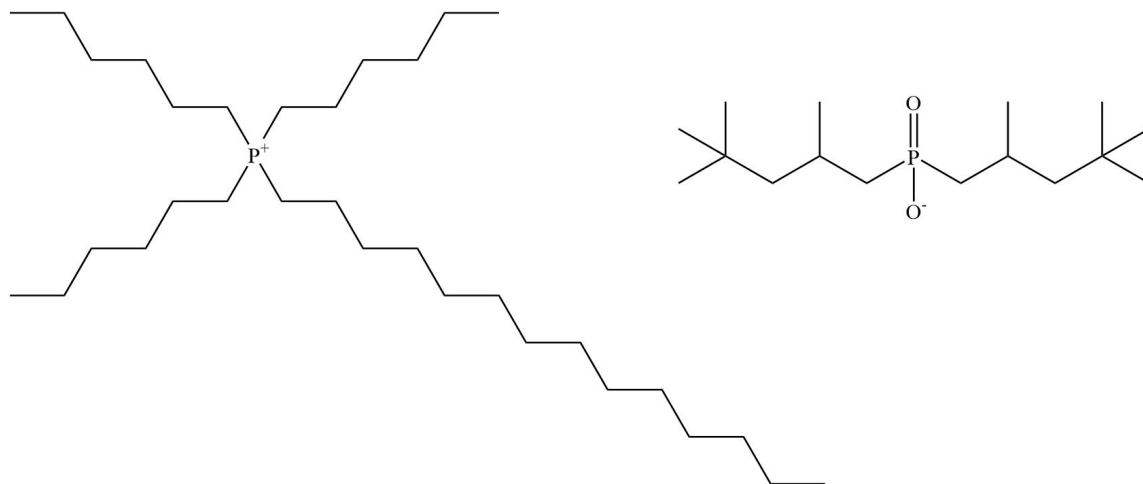
Figure 1: Structure of [P$_{6,6,6,14}$][DiOP]

1.43 g (0.0057 mol) bis(2,4,4-trimethylpentyl)phosphinic acid was mixed with 2.97 g (0.0057 mol) tetradecyl trihexyl phosphonium chloride in 5 g hexane. A solution of 0.32 g (0.0057 mol) KOH and 6 g distilled water was dropwise added into the reaction system and the mixture was stirred at room temperature for more than 4 h. The organic phase of the mixture was separated and washed with distilled water thrice. The solvent was removed by distillation and the product was dried by vacuum. The purity of the IL according to the NMR analysis is estimated to be around 99.5%. This IL was synthesized following a procedure reported in the literature.[40]

Figure 2: [C$_4$C$_1$Im][DMP]

Synthesis [C$_4$C$_1$Im][DMP]

57 g of distilled 1-butylimidazole was mixed with 50 ml ethyl acetate. 63.91 g (456 mmol, 53.40 ml) of dry trimethyl phosphate was added dropwise. Th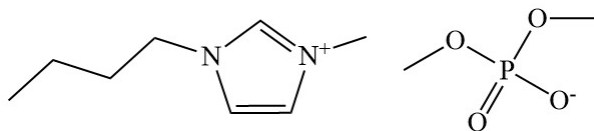e mixture was stirred under nitrogen atmosphere at 80°C for 20 h. 26 ml of distilled water were added. The solution was placed in the continuous extractor and extracted with toluene for at least 16 h in order to remove excess reactants. The aqueous phase was isolated, the water was removed and the ionic liquid dried at 80°C under vacuum. The product was a clear, colorless, oily liquid. The yield was 89.08 g (338.71 mmol, 74%). The IL estimated purity according to the NMR results is better than 98.0%. This IL was synthesized following a procedure reported in the literature.[41]

Gases Studied

The gases ethane, ethylene and propane used in the gas solubility measurements were supplied by Air Liquide at a level of purity of 99.95%. The propylene used in gas solubility measurements was supllied by Messer with a level of purity of 99.5%.

For the measurement of nuclear magnetic resonance spectra and the determination of the self-diffusion coefficients, ethylene (99.9% purity), ethane (99% purity) and propylene (99.5% purity) gases, supplied by BOC were bubbled into the ionic liquid.

All gases were used as received from the manufacturer.

Structural Characterization

The $[C_4C_1Im][DMP]$ and $[P_{6,6,6,14}][DiOP]$ IL samples were synthesized in the QUILL Research Centre. After synthesis they were characterized by NMR (400 and 600 MHz Bruker NMR), mass spectrometry (Waters Xevo -G2-XS Q-Tof) and elementary analysis (Perkin Elemer 2400 series 2). Both ILs were dried before use, and analysed *via* Karl Fischer (899 Coulometer, Metrohm).

^{1}H, ^{13}C and ^{31}P NMR spectra were also performed in ENS Lyon and confirmed the purity of the $[C_4C_1Im][DMP]$ and $[P_{6,6,6,14}][DiOP]$ ionic liquid samples used in the density, viscosity and gas solubility measurements. The ionic liquid samples used in the experiments were first dried and degassed under primary vacuum. The NMR spectrum was recorded on a Bruker Avance 400 MHz spectrometer at 298 K. The chemical shifts were referenced against the residual NMR solvent signal.

Density and viscosity measurements

The densities of the samples were measured in the temperature range 293–343 K and at atmospheric pressure in an Anton Paar DMA 5000M densimeter. The accuracy and precision of the densimeter were tested before the measurements with certified ultra-pure water and S3 density reference standard. The precision of the density results were estimated to be in the order of magnitude of $0.01\,kg \cdot m^{-3}$ and the accuracy is estimated to be better than $0.01\,\%$. Temperature is controlled to within $\pm 0.001\,K$.

The viscosity measurements were performed with an Anton Paar rolling ball viscosimeter Lovis 2000 ME at temperatures between 293–343 K. The set of 1.8 mm capillary and stainless steel ball of the Lovis 2000 ME viscosimeter was calibrated prior to the measurements at 298 K and 333 K at the angles 20–70° using the N100 standard oil reference. The accuracy and precision of the viscosity measurements were tested with N26 standard reference for viscosities in the range 11–$40\,mPa \cdot s$ and with N415 standard reference for viscosities in the range 30–$1100\,mPa \cdot s$. Considering the tests performed, the accuracy and precision of

the viscosity measurements are estimated to be better than 1.5% and 0.30%, respectively. Temperature is controlled to within ± 0.01 K. All the reference standards used in the calibration and test of the desimeter and viscosimeter were acquired from Paragon Scientific with exception of the certified ultra-pure water, which was supplied by Anton-Paar.

The ionic liquids were dried under vacuum (10 Pa) before the density and viscosity measurements at mild temperatures (310–318 K) for at least 4 days. The amount of water contained in each ionic liquid after the drying process was determined by a coulometric Karl Fisher titrator (Metler Toledo C20S using Hydranal Coulomat E as reagent). Using this drying methodology, the water amount was found to be always lower than 300 ppm. Nevertheless, as both the densimeter and the viscometer are open to atmosphere, some minor increase of the water content may occur during the sample transfer or the measurement.

Thermal analysis

The thermal behaviour and the temperatures of phase transition of both ionic liquids were evaluated in a differential scanning calorimeter (TA instruments, Q2000) using hermetically sealed aluminium crucibles, samples of about 20 mg, and a constant flow of nitrogen (50 mL/min). During the thermal analysis, each sample was cooled from 293 K to 203 K, at a rate of 5 K/min, and maintained at 203 K for 5 minutes. The samples were then heated to 323 K and maintained at 323 K for 5 minutes. This cycle was repeated $3\times$ (each cycle started now at 323 K, instead of 293 K). For $[P_{6,6,6,14}][DiOP]$, a modulated differential scanning calorimetry analysis was completed. The same pan set up was used and the measurement proceeded with a decrease of the initial temperature to 183 K followed by a temperature increase at a rate of 10 K/min. An amplitude of the temperature modulation (1.0 K), and a modulation period of 30 s were imposed.

The thermal stability of both ionic liquids was evaluated in a thermogravimetric analyzer (TA instruments, Q5000). Using platinum-HT pans with 40 mg of sample and constant nitrogen flow of 20 mL min^{-1}). Each ionic liquid sample was heated from 303–873 K at a rate

of $10\,\mathrm{K/\,min}$.

Gas absorption measurements

In this work, the gas solubility of ethane, ethylene, propane and propylene in $[\mathrm{C_4C_1Im}][\mathrm{DMP}]$ and $[\mathrm{P_{6,6,6,14}}][\mathrm{DiOP}]$ was measured using a volumetric isochoric saturation method. These measurements were performed in an in-house built equipment [42,43] in the temperature range 303–343 K and at pressures up to 1 bar. An independent experiment of the absorption of propane in the ionic liquid $[\mathrm{C_4C_1Im}][\mathrm{DMP}]$ at 303.16 K was also performed *via* gravimetric method using an Intelligent Gravimetric Analyzer (IGA001) from Hiden Analytical in the 0.5–2.5 bar pressure range.

In the isochoric gas absorption method, the quantity of gas absorbed is calculated from the difference between two pressure-volume-temperature (pVT) measurements. First, a known amount of gas, n_g^{tot}, is precisely determined from the accurate measurement of its pressure and temperature (p_{ini} and T_{ini}) when introduced in a gas bulb, with a previously calibrated volume V_{ini} and part of the equilibrium cell.

$$n_g^{\mathrm{tot}} = \frac{p_{\mathrm{ini}}(V_{\mathrm{ini}})}{Z(p_{\mathrm{ini}}, T_{\mathrm{ini}})RT_{\mathrm{ini}}} \tag{1}$$

where Z is the compressibility factor of the gas, calculated to the level of the second virial coefficient from the data compiled by Dymond *et al.* [44]

The second measurement of the temperature and pressure is performed when the thermodynamic equilibrium between the gas and a precise quantity of degassed ionic liquid is attained. The amount of non-dissolved gas remaining in the cell, n_g^{vap}, is calculated as:

$$n_g^{\mathrm{vap}} = \frac{p_{\mathrm{eq}}(V_{\mathrm{tot}} - V_{\mathrm{liq}})}{Z(p_{\mathrm{eq}}, T_{\mathrm{eq}})RT} \tag{2}$$

where p_{eq} and T_{eq} are the pressure and temperature at equilibrium and V_{tot} and V_{liq} are the total volume of the equilibrium cell and the volume occupied by the ionic liquid, respectively.

As explained in a previous work, [42] we consider that: i) the volume of the liquid phase does not change upon the dissolution of the gas; ii) the quantity of ionic liquid in the liquid phase, $n_{\text{IL}}^{\text{liq}}$, remains constant, as its vapour pressure is negligible in the temperature range covered. These approximations were proven to have a negligible effect on the accuracy of the gas absorption measurements. [43] The amount of gaseous solute absorbed by the ionic liquid sample, $n_{\text{g}}^{\text{liq}}$, is then calculated as:

$$n_{\text{g}}^{\text{liq}} = n_{\text{g}}^{\text{tot}} - n_{\text{g}}^{\text{vap}} \tag{3}$$

In this publication, the solubility will be expressed as the solute mole fraction at a constant partial pressure of gas x_2 with an associated Henry's law constant, K_{H}, both calculated from the amount of gaseous solute absorbed by the ionic liquid sample, as follows:

$$x_2 = \frac{n_{\text{g}}^{\text{liq}}}{n_{\text{IL}}^{\text{liq}} + n_{\text{g}}^{\text{liq}}} \tag{4}$$

$$K_{\text{H}} = \lim_{x_g \to 0} \frac{\phi_{\text{g}} p}{x_{\text{g}}} \tag{5}$$

During the gas absorption measurements we noticed an small absorption of the hydrocarbon gases in the Apiezon H lubricant used in the glass joints of our isochoric saturation apparatus. This absorption is not negligible if we want to maintain the high accuracy of our solubility measurements. An experimental assessment of this absorption was possible and so a correction could be made, on the basis of experimentally determined behaviours, to prevent systematic deviations in the solubility. Details on the methodology used to correct this effect is given in the supplementary information.

The gravimetric experiment was done following a procedure described before. [45] A sample of ionic liquid of around 100 mg was loaded in the sample holder and sealed in the measuring cell before being degassed and dried first by a primary vacuum (up to a level of 200 Pa) with a membrane pump (Vacuubrand, MD1) and then a turbo pump (Edwards, EXT75DX)

typically to about 10^{-6} Pa. The drying and degassing step was performed at $318\,\mathrm{K}$ for a time of $46\,\mathrm{h}$. During the evacuation of the absorption chamber, the sample mass decreased slowly until stabilization, due to the decrease of gas and water content in the sample. The sample mass remaining at the end of the evacuation step was recorded as the dry mass of the sample. The temperature of the apparatus is controlled into two different areas: the balance and the sample chamber. A platinum resistance sensor (Pt100) was used to monitor the temperature inside the absorption chamber and in the balance with an accuracy of $\pm\,0.1\,\mathrm{K}$. During the experiments, the temperature of the absorption chamber is kept constant by an external water jacket connected to an external water thermostat (Grant Scientific, GR150).

The gas sorption measurements were conducted in static mode, in which a specified gas pressure is maintained above the sample, preventing oscillating buoyancy effects due to the gas flow. Once the temperature is stable, the admission/exhaustion valves are automatically opened or closed to attain the pre-programmed pressures. The manometer used is a piezo-resistive strain gauge (GE Sensing, UNIK 5000) with an accuracy of $\pm\,0.04\%$ full scale. The Intelligent Gravimetric Analyzer regulates the temperature and pressure continuously, while recording the sample weight. Analysing the data obtained in real-time allows the prediction of the trend towards equilibrium and the determination of the equilibrium point for each isotherm based on the defined criteria. The end-point for each isotherm was thus determined using the IGASwin software. To guarantee sufficient time for gas–liquid equilibrium, the samples were kept at the set-point for at least $3\,\mathrm{h}$ with a maximum timeout of $10\,\mathrm{h}$. The percent relaxation used as an end point for the real-time analysis was $99.5\,\%$, the minimum weight change for real-time analysis being set at $1\,\mu\mathrm{g}$. The acceptable average deviation of the model from the acquired data was set at $5\,\mu\mathrm{g}$, and the target interval for weight acquisition at $0.5\,\mu\mathrm{g}$. The temperature variation observed during an isotherm was lower than $0.1\,\mathrm{K\,min^{-1}}$. After attaining the equilibrium, the pressure is raised to attain the next equilibrium point of the programmed sorption isotherm. This process is then reversed and a series of desorption steps are made, obtaining a complete absorption/desorption isotherm.

The mass of gas absorbed, m_g, at a given temperature and pressure, is obtained from the raw weight data, m_{reading}, by:[45]

$$m_{\text{reading}} = m_0 + m_s + m_g + m_g^{\text{EP}}$$
$$- \sum_i \frac{m_i}{\rho_i} \rho_g(T_i, p) + \sum_j \frac{m_j}{\rho_j} \rho_g(T_j, p) - \frac{m_s}{\rho_s(T_s)} \rho_g(T_s, p) \quad (6)$$

where m_0 ($\approx \pm 10^{-4}$ to $\pm 10^{-3}$mg) is a small residual mass read after the tare with the empty pan at zero pressure, m_s is the mass of degassed sample, m_g^{EP} is the mass effect resulting from adsorbed gas on the balance components (determined by performing a blank measurement with the empty pan) and the sums with the i and j subscripts represent the buoyancy effects on the sample and counterweight sides, respectively. It was considered that the buoyancy differences associated with changes in sample volume due to the (small) amount of dissolved gas were negligible. $\rho_s(T_s)$ is the density of the ionic liquid sample at the measurement temperature (303.16 K) and $\rho_g(T_s, p)$ is the gas density at the equilibrium temperature and pressure. The density of the gas was calculated using the REFPROP v.7 program available in the NIST ChemistryWebBook. More details on the the gravimetric experiments, the setup and all the considerations were extensively described previously by Avila *et al.*[45]

NMR spectroscopy

We have used nuclear magnetic resonance (NMR) spectroscopy to investigate the nature of the gas-ionic liquid interactions. A deuterated dimethylsulfate solvent capillary was inserted into the standard Wilmad NMR 5 mL tubes and was used as reference. The NMR tube is then filled with dried ionic liquid and sealed with 5 mm thin-walled rubber septa tube cap. The gases were bubbled through the $[C_4C_1Im][DMP]$ and $[P_{6,6,6,14}][DiOP]$ ionic liquids *via* an inlet needle, excess gas being removed through an outlet needle. To allow a slightly higher gas pressure, the outlet needle was removed just before the analysis of samples. No precise measure of the flow rate or pressure of gas in the NME tube was measured. ^{1}H, ^{13}C and ^{31}P

single dimensional spectra were performed to confirm the existence of the gas signals and to evaluate the gases' relevant chemical shifts.

2D spectra were performed in a Bruker 600 MHz spectrometer to evaluate the existence of proximity in space and specific interactions: NOESY was used for determining which signals arise from protons that are close to each other in space, even if they are not bonded and DOSY was used to separate the NMR signals of different species according to their diffusion coefficients. From DOSY NMR experiments, the self-diffusion coefficients were determined for the pure ionic liquid and for the ionic liquids containing each of the gases. [46,47] The self-diffusion coefficients for the cation and anion can be determined in this case due to the overlapping of anion and cation peaks, the self-diffusion coefficient of the cation was used. All spectra were obtained at 298 K.

Results & Discussion

When studying the thermal stability of $[C_4C_1Im][DMP]$, we have observed by thermogravimetric analysis an initial small mass loss occurring below 120°C. This loss is likely to be due not only to the thermal degradation of the sample but also to the evaporation of water and other volatiles. [48] The extrapolated onset of the decomposition temperature was approximately 299°C. The decomposition of this ionic liquid was found to occur in three steps, with the first step being responsible for over 69% of the mass loss and the second for 18%. The second step of the decomposition started around 320°C and the third just above 480°C. Our results are close to those of Clough *et al.* that reported an extrapolated onset decomposition temperature of 282°C for the same ionic liquid using a comparable TGA method. [49] The differences encountered are expected as the synthetic methodologies reported by the authors are different from those used in this work. Although in both cases no major impurities were detected by NMR, the ionic liquid used herein is colourless while Clough *et al.* describe a light yellow, free-flowing liquid. In another thermal stability study, this time referencing

the long term stability of $[C_4C_1Im][DMP]$, it was reported that this ionic liquid was stable at 120°C for over a period of 60 hours, but there was no mention of an extrapolated onset decomposition temperature.[50]

In the case of $[P_{6,6,6,14}][DiOP]$ we observed a mass loss, attributed to the start of the thermal decomposition, at around 200°C and the extrapolated onset decomposition temperature was determined to be approximately 361°C with a one step degradation pathway. For the same ionic liquid, Silva *et al.*[51] and Yu *et al.*[52] reported an extrapolated decomposition temperature of 369°C and 366°C, both works reporting a one step degradation path. These values are close to the ones reported here, the larger degradation temperature reported by Silva *et al.* being probably due to the higher heating rates used.

The comparison between the thermal stability of the two ionic liquids is difficult, due to the differences in the structures of the cations and anions.[53] However, it is worth mentioning that their extrapolated onset decomposition temperatures are within what is expected for these families of ionic liquids.[48] The decomposition of phosphonium-based ionic liquids seems to follow a S_N2 mechanism to form a ylide, so the higher decomposition temperature of $[P_{6,6,6,14}][DiOP]$ can be at least partially justified by the presence of longer alkyl chains that might hinder the access to the CH_2 groups in the α position of the alkyl chains of the phosphonium cation, particularly in presence of a very sterically hindered anion.[54]

The glass transition temperature of $[C_4C_1Im][DMP]$, determined using DSC, was found at -64.21°C, comparable to -64.70°C reported by Clough *et al.*[49] In the case of $[P_{6,6,6,14}][DiOP]$, only a small change in the baseline of the DSC thermogram was noticed around -20°C when using the same method as for $[C_4C_1Im][DMP]$. Differently, for other phosphonium ionic liquids based on the $[P_{6,6,6,14}]^+$ cation, the glass transition temperature is typically observed in the range from -80°C to -60°C.[55] When using modulated DSC with an initial temperature of -90°C, a glass transition temperature was recorded at around -71.83°C, the event at around -20°C being reproducible when the measurement was repeated. This event could be due to impurities present, such as water as there are evidences of similar events

at around 0°C. This shift has been attributed to the hindered rotation of the ion pair that ought to its morphology moves more easily with increased temperature.[55] All the curves thermograms can be found in supporting information.

The densities of the two ionic liquids, $[C_4C_1Im][DMP]$ and $[P_{6,6,6,14}][DiOP]$, measured between 293–343 K and at atmospheric pressure are reported in the supplementary information together with their calculated molar volumes. The data were fitted to linear functions of temperature, the average relative deviation of the fits being always better than 0.01%:

$$\rho[[C_4C_1Im][DMP]]/kg \cdot m^{-3} = 1354 - 0.656 \times (T/K) \tag{7}$$

$$\rho[[P_{6,6,6,14}][DiOP]]/kg \cdot m^{-3} = 1060 - 0.588 \times (T/K) \tag{8}$$

As expected, in light of the relative sizes of the ions, the $[P_{6,6,6,14}][DiOP]$ ionic liquid presents a molar volume significantly higher than $[C_4C_1Im][DMP]$. This points towards a lower cohesive energy density for the phosphonium salt.[56] This cohesive energy density is a measure of the difficulty of disrupting the intermolecular interactions between the molecules of a solvent in the liquid phase, per unit volume, and can be calculated as:

$$ced = \frac{\Delta_{vap}H - RT}{V_m} \tag{9}$$

where $\Delta_{vap}H$ is the vaporization enthalpy of the solvent and V_m its molar volume.

When considering conceptually that the dissolution of a solute consists on two steps, the first being the creation of a large enough cavity in the solvent and the second the introduction of the solute in the cavity, the cohesive energy is directly related with the former. Ionic liquids are known to vaporize as ion pairs and so their cohesive energy can be regarded as a measure of the energy of interaction between ion pairs. It is not possible to calculate accurately

19

the cohesive energy density of the ionic liquids studied in this work as no data on their enthalpy of vaporization was reported. Nonetheless, Lovelock,[56] by assuming that all the ionic liquids have enthalpies of vaporization of the same order of magnitude, could report a linear correlation of the cohesive energy of different ionic liquids with the inverse of their molar volume. Using this linear relation,[56] we could estimate the cohesive energy densities of $[C_4C_1Im][DMP]$ and $[P_{6,6,6,14}][DiOP]$ as $\approx 640\,J\cdot cm^{-3}$ and $\approx 167\,J\cdot cm^{-3}$, respectively. This indeed indicates a looser ion packing in the liquid state of $[P_{6,6,6,14}][DiOP]$, which might be favourable for the solubility of weakly interacting gases.[57]

The experimental viscosity of the ionic liquids $[C_4C_1Im][DMP]$ and $[P_{6,6,6,14}][DiOP]$ is reported in the supporting information and represented in Figure 3 as a function of temperature. The temperature dependence of the experimental data evidenced a systematic deviation from an Arrhenius-like behaviour and so in order to correct this deviation, the temperature dependence of the viscosity of both salts was described using a Vogel-Fulcher-Tammann (VFT) equation:

$$\eta = \eta_\infty \times \exp(\frac{B}{T - T_0}) \tag{10}$$

Table 1: Vogel-Fulcher-Tammann equation parameters and associated uncertainty at a 95% level of confidence obtained from the fitting of viscosity ($\eta/mPa\cdot s$) as a function of temperature (T/K) between 293 and 343 K and at 0.1 MPa, together with the average relative deviation of the experimental data points to the fitting.

	$\eta/mPa\cdot s$		
	$(\eta_\infty \pm \sigma)/mPa\cdot s$	$(B \pm \sigma)/K$	$(T_0 \pm \sigma)/K$	ARD / %
$[C_4C_1Im][DMP]$	0.065 ± 0.006	1115 ± 22	177 ± 1	0.2
$[P_{6;6;6;14}][DiOP]$	0.030 ± 0.065	1811 ± 813	127 ± 42	0.4

where η_∞, B and T_0 are the adjustable parameters of the fitting equation that are reported

in Table 1. Both salts are viscous liquids, 10^2 to 10^3 times more viscous than water at ambient temperature (0.89 mPa·s at 298 K[58]). From the values adjusted to the VTF fitting, it is clear that the viscosity of both ionic liquids are of the same order of magnitude (10^{-5} Pa·s) of most molecular liquids at infinite temperature (10^{-5} Pa·s to 10^{-6} Pa·s).[59] This was expected, since the higher viscosity of ionic liquids is commonly associated to their high molecular weights and stronger intermolecular interactions. As the temperature increases, the contribution arising from intermolecular interactions will decrease, decreasing the viscosity and the difference between the viscous behaviour of different types of liquids. The energy barrier of the ionic liquids to shear stress, E, at different temperatures can be calculated from:

$$E = R\frac{\partial[ln(\eta)]}{\partial(1/T)} = R\frac{B}{\frac{(T_0)^2}{T^2} - \frac{2T_0}{T} + 1} \tag{11}$$

Using this equation, the values of the energy barrier of $[C_4C_1Im][DMP]$ and $[P_{6,6,6,14}][DiOP]$ to shear stress for each experimental temperature were derived and are plotted in Figure 3. We observe that the energy barrier to viscous flow is higher for $[C_4C_1Im][DMP]$, which is in agreement with a higher cohesive energy density as estimated from its molar volume.

The experimental solubilities of ethane, ethylene, propane and propylene in $[C_4C_1Im][DMP]$ and $[P_{6,6,6,14}][DiOP]$ between 303 K and 343 K are listed in supporting information. The volume of ionic liquid in the equilibrium cell, V_{liq}, was obtained from the gravimetric determination of the amount of ionic liquid added and from the experimental density of the pure ionic liquid, reported in the supplementary information. The calculated Henry's law constants (K_H / 10^5 Pa) were fitted to a power series in temperature (T/ K),
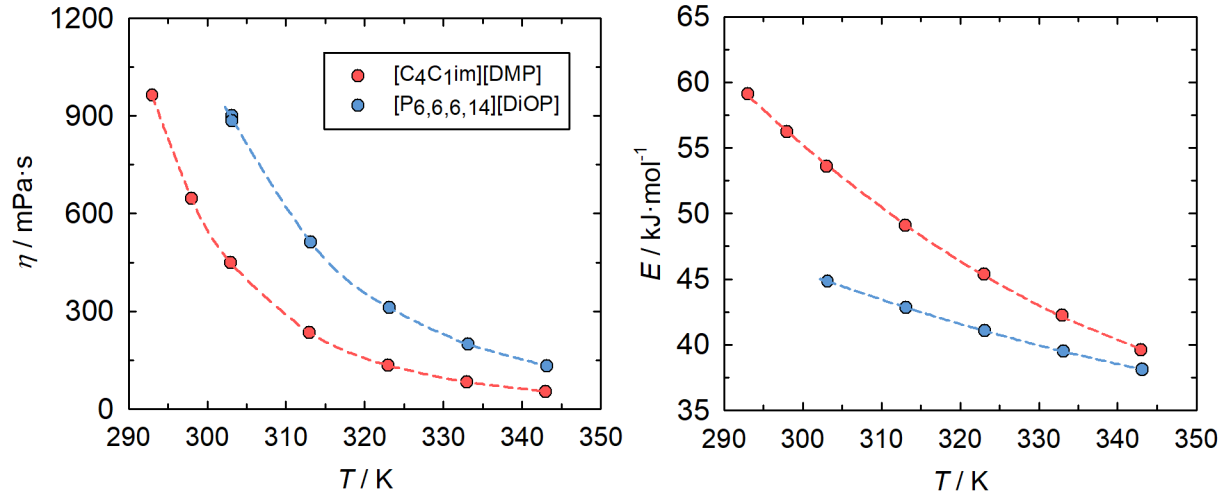
Figure 3: Graphical representation of the viscosity of the studied ionic liquids (on the left) and the derived energy barrier (on the right) as a function of the experimental temperature. The dashed lines are just guides to the eyes.

as presented in eq (12). The A_i coefficients are listed in supporting information.

$$ln(K_H) = \sum_{i=0}^{n} A_i \times (T)^{-i} \tag{12}$$

The mole fraction solubility of all the studied gases in $[C_4C_1Im][DMP]$, is of the order of 10^{-3}, which correspond to 1 to 20 molecules of gas per 1000 ion pairs at 313 K and 0.1 MPa. As illustrated in Figure 4, the ionic liquid $[P_{6,6,6,14}][DiOP]$ shows better capacity to absorb all the studied gases, with up to 169 molecules of propane per each 1000 ion pairs at 313 K and 0.1 MPa.$[C_4C_1Im][DMP]$ showed higher capacity to absorb olefins than paraffins, while $[P_{6,6,6,14}][DiOP]$ showed the opposite behaviour.

The solubility of the studied gases has a direct relation with the Gibbs free energy of solvation, as described in eq (13). The Gibbs energy of solvation can be described as the change in Gibbs energy when the solute is transferred, at constant temperature and pressure, from the pure perfect gas state to the solvent at infinite dilution.

$$\Delta_{sol}G^{\infty} = RT\ln\left(\frac{K_H}{p^0}\right) \tag{13}$$
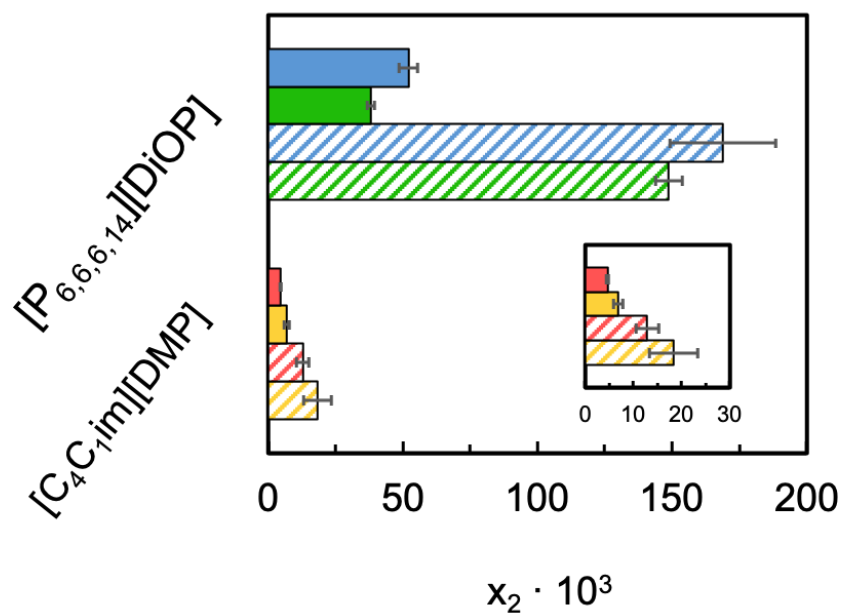
22

Figure 4: Mole fraction solubility of the studied gases in $[C_4C_1Im][DMP]$ and $[P_{6,6,6,14}][DiOP]$ at 0.1 MPa and 313 K: blue, solubility of ethane and propane in $[P_{6,6,6,14}][DiOP]$; green, solubility of ethylene and propylene in $[P_{6,6,6,14}][DiOP]$; magenta, solubility of ethane and propane in $[C_4C_1Im][DMP]$; yellow, solubility of ethylene and propylene in $[C_4C_1Im][DMP]$; full coloured bars, solubility of ethane and ethylene; patterned bars, solubility of propane and propylene. The mole fraction solubility of ethane and ethylene in $[P_{6,6,6,14}][DiOP]$ was calculated from the data reported by Liu *et al.*[60]

To better interpret the differences in solubility between the different gases and ionic liquids, it is helpful to look at the interplay between the enthalpic and entropic contributions to the solvation process, which can be obtained by calculating the derivative of the Gibbs energy with respect to the temperature, as follows:

$$\Delta_{sol}H^{\infty} = -T^2 \frac{\partial}{\partial T}\left(\frac{\Delta_{sol}G^{\infty}}{T}\right) = -RT^2 \frac{\partial}{\partial T}\left[\ln\left(\frac{K_H}{p^0}\right)\right] \tag{14}$$

$$\Delta_{sol}S^{\infty} = \frac{(\Delta_{sol}H^{\infty} - \Delta_{sol}G^{\infty})}{T} = -RT\frac{\partial}{\partial T}\left[\ln\left(\frac{K_H}{p^0}\right)\right] - R\ln\left(\frac{K_H}{p^0}\right) \tag{15}$$

The calculated values for the thermodynamic properties of solvation of the studied gases in $[C_4C_1Im][DMP]$ and $[P_{6,6,6,14}][DiOP]$ are listed in supplementary information. In Figure 5 are depicted the entropic and enthalpic contributions to the solvation of each of the studied gases in both ionic liquids at 313 K. In all cases, the solvation is ruled by the entropic term, which plays an unfavourable contribution to the process. The entropic term also seems to explain the higher solubility of all the studied gases in $[P_{6,6,6,14}][DiOP]$, since all the gases seem to have a less unfavourable entropic contribution. Although Stassen et al.[61] have pointed that interactions in ILs might explain entropic-driven solvation, in this work it was not possible to find clear evidences of gas-ionic liquid interactions as the enthalpy of solvation of the gases studied is similar in all the studied pairs.

The uncertainty associated to the thermodynamic properties renders difficult to clearly distinguish between the role of the enthalpy and entropy in the preferential solubility of paraffins or olefins in $[P_{6,6,6,14}][DiOP]$ or in $[C_4C_1Im][DMP]$. However, if the alkenes were able to establish more specific interactions (as π-interactions) with $[C_4C_1Im][DMP]$, for example, the solvation of the alkenes would be expected to be more exothermic. A higher endothermic contribution, capable of surpassing the enthalpic effect of eventual specific interactions, would not be expected as the energetic contribution caused by the creation of a cavity in the liquid salts would be similar as ethane and ethylene have similar sizes, both with van der Waals

radii of 2.95 Å and 2.84 Å, as well as propane and propylene with van der Waals radii of 3.30 Å and 3.20 Å. Based on these assumptions, the entropic term is the most important to explain the solubilities measured.
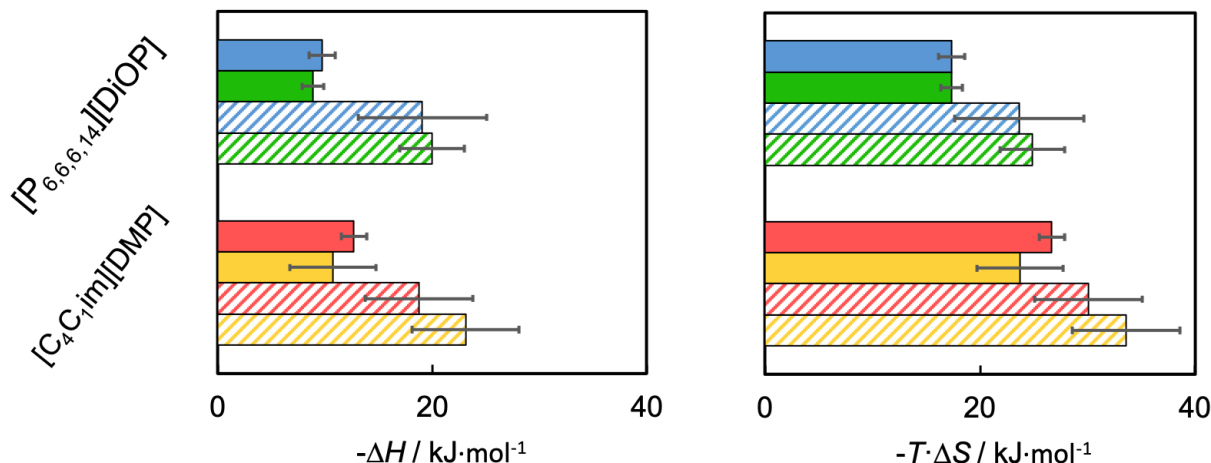

Figure 5: Graphic representation of the enthalpic and entropic contributions to the solubility of the studied gases in $[C_4C_1Im][DMP]$ and $[P_{6,6,6,14}][DiOP]$ ionic liquids, at 0.1 MPa partial pressure and 313 K: blue, solubility of the ethane and propane in $[P_{6,6,6,14}][DiOP]$; green, solubility of ethylene and propylene in $[P_{6,6,6,14}][DiOP]$; magenta, solubility of the ethane and propane in $[C_4C_1Im][DMP]$; yellow, solubility of ethylene and propylene in $[C_4C_1Im][DMP]$; full coloured bars, solubility of the ethane and ethylene; patterned bars, solubility of the propane and propylene. Enthalpic and entropic contributions to the solubility of ethane and ethylene in $[P_{6,6,6,14}][DiOP]$ calculated from the data reported by Liu *et al.*[60]

As the concentration of the gases is low enough, they can be considered as infinitely diluted in the ionic liquids with absence of solute-solute intermolecular interactions in the solutions. In accordance, the solvation process can be interpreted as an interplay between the penalty of creating a cavity in the solvent and the solute-solvent interactions. Since no evidence of specific interactions between the gases and the ionic liquids is evidenced in the thermodynamic properties of solvation, an understanding of the cavitation mechanism might contribute to the explanation of the gas solubility.

The mechanism of creation of a cavity in a solvent has been considered to depend on the interplay between the internal pressure of the solvent and its cohesive energy density.[62] The internal pressure of a solvent (P_i) is related with its capacity to reorganize and create cavities

without breaking the intermolecular interactions. In other words, the internal pressure describes the change in the solvent internal energy when the intermolecular distance increases, without disruption of the interactions. The ratio between the internal pressure and the cohesive energy density are characteristic of each solvent. Solvents with $P_i/ced \leq 0.80$ are usually denominated as "stiff" or "tight" solvents since its cohesive energy density is superior to its internal pressure. Water and light alkanols are examples of "stiff" solvents. Solvents for which the internal pressure is superior to the cohesive energy density, $P_i/ced \geq 1.20$, are usually considered "loose" solvents. The solvation of small solutes (radii ≤ 3) in water is often used to exemplify the interplay between ced and P_i. Water presents a much higher ced than P_i, which results in a $P_i/ced = 0.07$. Therefore, the "creation of a cavity" for the solvation of a small molecule in water will preferentially occur through the re-orientation of its without sacrificing the intermolecular interactions. Otto[62] suggests that as long as the radius of the solute is inferior to 10 Å, the water hydrogen bonds may be maintained. For bigger solutes, some water hydrogen bonds would have to be sacrificed.

Otto[62] has reported the existence a correlation between the Gibbs energy of solvation of ethane and propane in both non-polar and polar molecular liquids with a combination of $0.45ced + 0.55P_i$ for ethane and $0.5ced + 0.5P_i$ for propane. These correlations clearly demonstrate a higher contribution of ced in the case of the solvation of bigger solutes. Specifically, it was shown that for solutes with radius larger than 3 Å, the ced becomes the biggest contributor to the Gibbs energy of solvation. The gases studied in this work present van der Waals radii of 2.95 Å (ethane) to 3.30 Å (propane). If we assume that their Gibbs energy of solvation can be estimated following the correlations described above for molecular solvents, both ced and P_i would contribute by approximately 50%, or that the ratio P_i/ced determines the solubility of these gases in the ionic liquids. Unfortunately, the internal pressure of the ionic liquids in this study is unknown. However, a review[63] on the topic has shown that the internal pressure of ionic liquids is 50% to 70% smaller than its cohesive energy densities, with P_i/ced ratios between 0.60 and 0.85, characteristic of associated or "tight"

liquids. The cohesive energy densities of the ionic liquids studied are comparable in magnitude to the cohesive energy density of n-butanol[63] $ced_{C_4H_9OH} = 493\,\mathrm{J \cdot cm^{-3}}$ or n-pentane[63] $ced_{C_5H_{12}} = 207\,\mathrm{J \cdot cm^{-3}}$. As ionic liquids generally present characteristics of "moderately tight" liquids, we can imagine that the creation of cavities to accommodate these solutes occurs primarily through the increase of the intermolecular distance in the solvent but without breakage of the intermolecular interactions. The less unfavourable solvation of all the gases studied in $[P_{6,6,6,14}][DiOP]$ suggests that this ionic liquid might have a higher P_i/ced ratio than $[C_4C_1Im][DMP]$.

To develop a good solvent for gas separation it is not only important to understand the capacity of absorption of the ionic liquids but also, the capacity to selectively absorb one gas over the other. As the studied gases present low levels of absorption in the studied ionic liquids, their activity coefficients in the liquid phase can be considered to be close to unity. This allows us to calculate an ideal gas selectivity, which should be comparable to the selectivity presented by the ionic liquids in a real gas mixture.

Given the fact that alkanes are more soluble in $[P_{6,6,6,14}][DiOP]$, whereas alkenes are more soluble in $[C_4C_1Im][DMP]$, in this work, the ideal selectivity will be calculated as the ratio of Henry's law constant between two gases (alkane/alkene) in a certain ionic liquid, as follows:

$$\alpha = \frac{K_{H,1}}{K_{H,2}} \tag{16}$$

where, $K_{H,1}$ and $K_{H,2}$ represent respectively the higher and lower Henry's law constants from the alkane/alkene gas pair. The obtained selectivity values in $[P_{6,6,6,14}][DiOP]$ and $[C_4C_1Im][DMP]$ are represented in Figure 6 at 313 K. Together with our data, the results by Liu *et al.*[60] were added to help determine the ideal selectivity of $[P_{6,6,6,14}][DiOP]$ for the ethane and ethylene separation. Despite the high uncertainties involved, from the analysis of the Figure 6 it seems that $[C_4C_1Im][DMP]$ has higher selectivity for both ethane/ethylene and propane/propylene separations. This is despite the fact that in this work, no evidence of specific interactions gas-solvent being found either the thermodynamics or in NMR analysis,

which might explain the somewhat similar selectivities found. Because of the uncertainly associated with the calculated selectivity, no definitive conclusions can be drawn regarding its variation with temperature in the two ionic liquids (see figure in supporting information). However, if gas-ionic liquid specific interactions were present, it would be expected that the selectivity would trend to decrease with increasing temperature. No evidence of this trend was found.
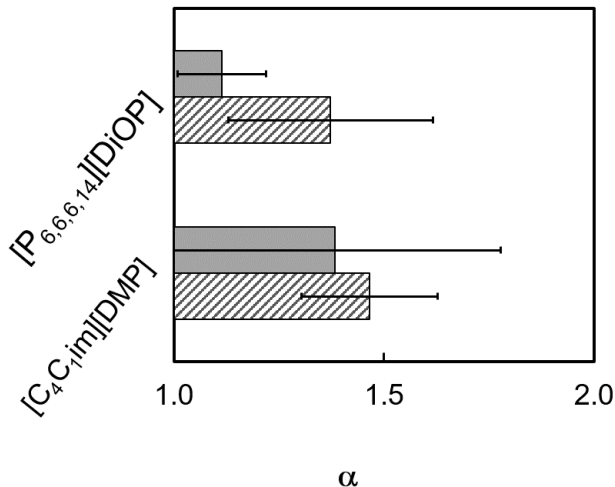

Figure 6: Ideal selectivity, α, for the alkane/alkene separation in the ionic liquids $[C_4C_1Im][DMP]$ and $[P_{6,6,6,14}][DiOP]$ at 313 K. Full coloured bar represents propane/propylene selectivity; patterned bar represents ethane/ethylene selectivity.

One- and two-dimensional NMR were used to characterise the two ionic liquids in the presence and absence of the gases, ethane, ethylene and propylene. Our goal was to investigate the effect of these gases in the self-diffusion coefficients and to search for evidences of the specific gas-ionic liquids interactions. To do this, ^{1}H, ^{13}C and ^{31}P NMR spectra were obtained of the pure ionic liquids, followed by the ^{1}H NMR spectra of their mixtures with each of the gases to detect the presence and variations in the chemical shifts of the protons of each solute in solution. All spectra can be consulted in the supplementary information. The proton chemical shifts for ethane, ethylene and propylene in a reference solvent, deuterated DMSO[64] and in the ionic liquids, $[C_4C_1Im][DMP]$ and $[P_{6,6,6,14}][DiOP]$ are compiled in Table

[2]. No significant chemical shifts of the gases' or ionic liquids' proton signals were observed

Table 2: Proton chemical shifts (ppm) for ethane, ethylene and propylene in deuterated DMSO,[64] $[C_4C_1Im][DMP]$ and $[P_{6,6,6,14}][DiOP]$. Ethane's protons presented as a CH_3 singlet, ethylene's protons as a CH_2 singlet and propylene as a CH_3 doublet of triplets, a CH_2 doublet of multiplets, a CH_2, doublet of multiplets, and a CH multiplet in this order.

	Ethane	Ethylene	Propylene
DMSO	0.82	5.41	1.68
			4.94
			5.03
			5.80
$[C_4C_1Im][DMP]$	0.74	5.32	1.61
			4.82
			4.91
			5.74
$[P_{6,6,6,14}][DiOP]$	0.83	5.31	1.65
			4.86
			4.94
			5.72

in the mixtures, an indication of the absence of strong specific gas-liquid interactions. The small chemical shifts shifts observed in gas' proton peak positions (around < 0.1 ppm) can be accounted by the different environments present in the two ionic liquids and between the solvents and the deuterated DMSO.

NOESY was used to determine which signals arise from protons that are close to each other in space, even when they are not bonded. In this study this could give indications on the proximity of the gases with certain sites in the ionic liquids. However, we observed no peaks along the area corresponding to the gases' chemical shifts (Figures 7, 8 and 9), signifying that there is no correlation between the gas' and the salts' proton peaks, an indication that there is no strong interaction or close proximity between the protons in the gases and in the ionic liquids. In fact, the only peaks observed correspond solely to the correlation between the ionic liquid's own protons.

DOSY NMR allows for the determination of the self-diffusion coefficients of the ionic liquids. Samples of $[P_{6,6,6,14}][DiOP]$ and $[C_4C_1Im][DMP]$ with different amounts of water
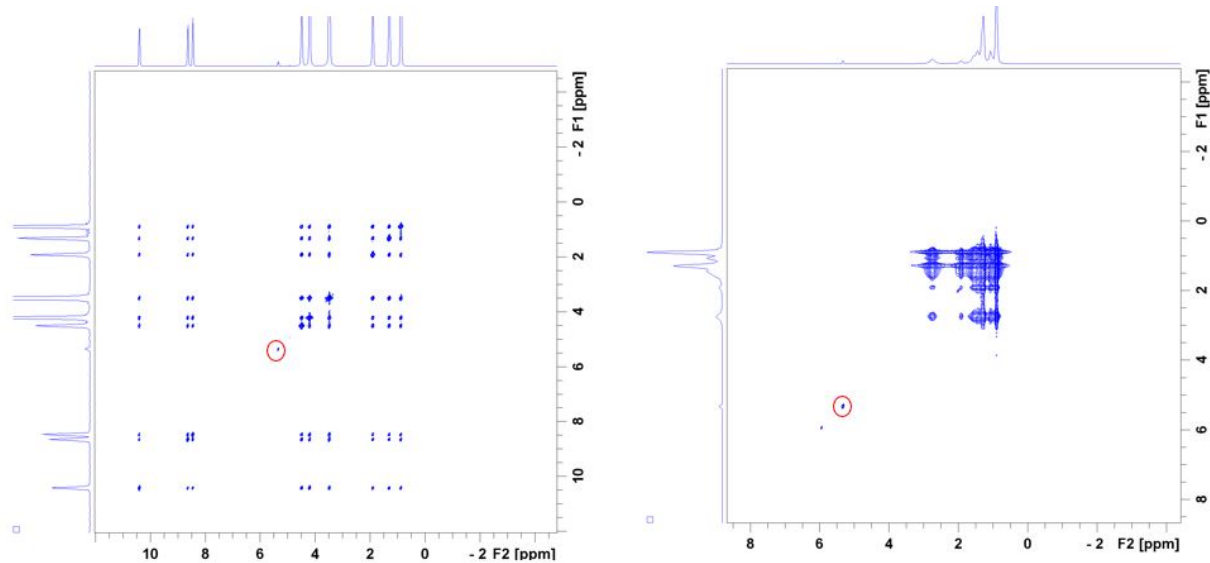
Figure 7: NOESY NMR of [C$_4$C$_1$Im][DMP] (left) and [P$_{6,6,6,14}$][DiOP] (right) containing ethylene. The ethylene peak is highlighted by the circles.
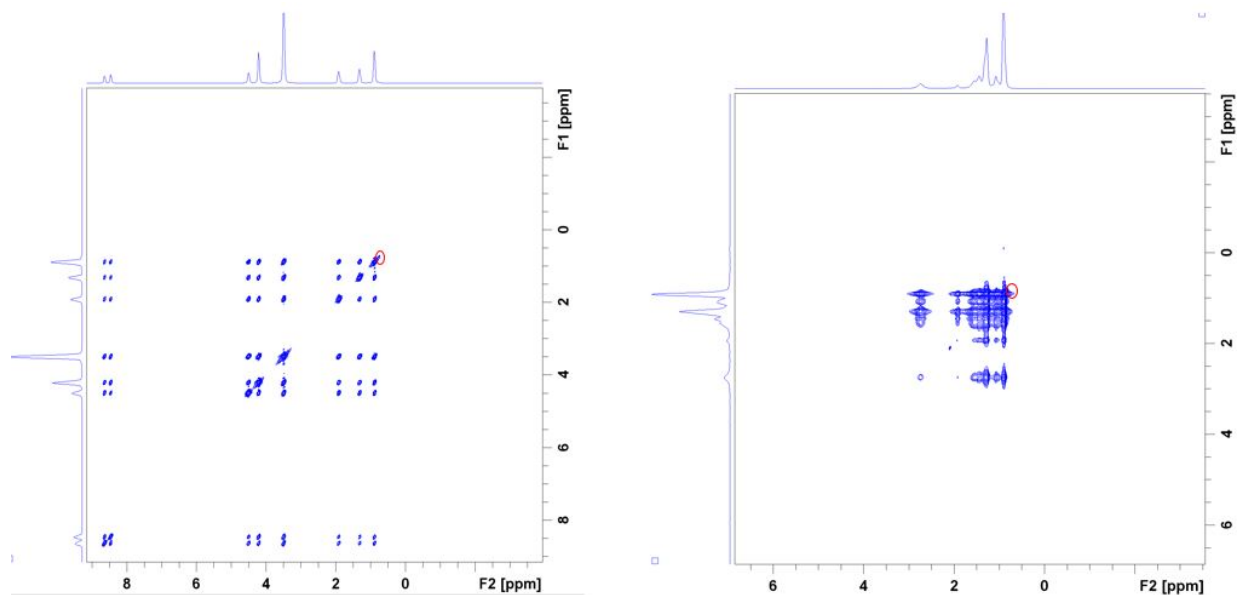

Figure 8: NOESY NMR with ethane bubbled through[C$_4$C$_1$Im][DMP] (left) and [P$_{6,6,6,14}$][DiOP] (right). The ethane peak highlighted by the circle in each case.
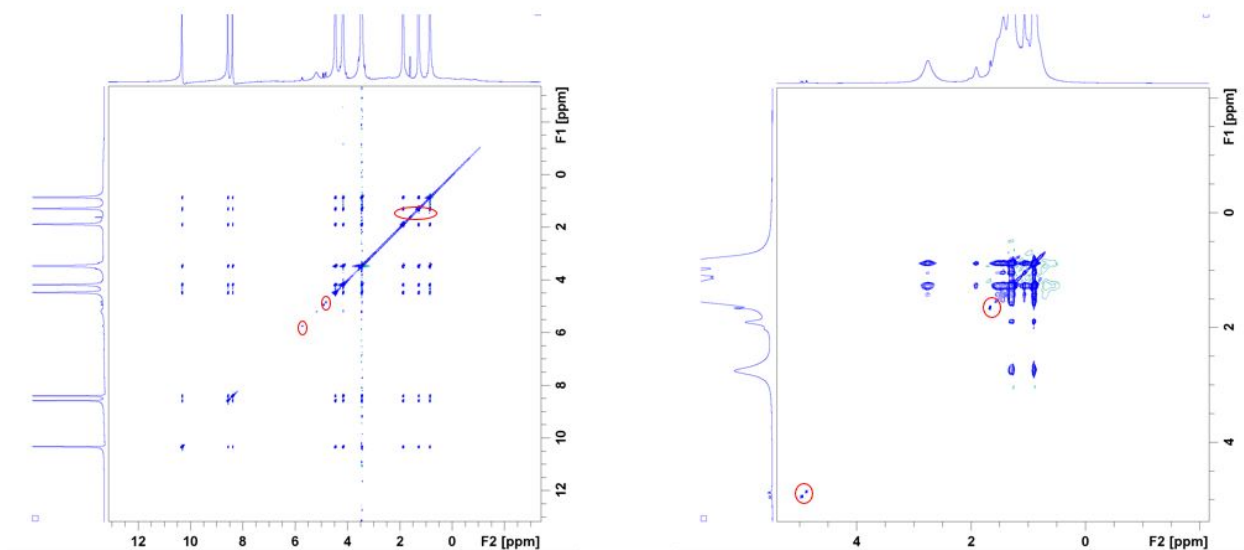
Figure 9: NOESY NMR with propylene bubbled through [C$_4$C$_1$Im][DMP] (left) and [P$_{6,6,6,14}$][DiOP] (right). The ethylene peak highlighted by the circle in each case.

were studied and the self-diffusion coefficients obtained are listed in Table 3 to 5, along with the results in the presence of the absorbed gases. For [C$_4$C$_1$Im][DMP], the self-diffusion coefficients of the cation and anion remained very similar. For [P$_{6,6,6,14}$][DiOP], there was an overlap of the ^{1}H spectra peaks for the cation and anion, making it difficult to differentiate them. In this case, a terminal CH$_3$ of the cation was used as the reference.

It is interesting to observe that the large difference in size of the cation in both ionic liquids is not reflected in a large difference in their self-diffusion coefficients, even with a large differences in their viscosities. This effect has been systematically explored in a series of publications by Watanabe's group in order to establish a relationship between microscopic ion dynamics, structures and the physicochemical properties of different families of ionic liquids. [65–67] Based on these, one possible explanation for the results observed herein is that a stronger interaction or proximity between the pair [C$_4$C$_1$Im][DMP] is expected in comparison with [P$_{6,6,6,14}$][DiOP], due to the stronger coordination ability, availability and higher charge density of the ions in the first ionic liquid. As explained before for the viscosity, this means ultimately that [C$_4$C$_1$Im][DMP] will likely have a stronger ion-pairing/aggregation than [P$_{6,6,6,14}$][DiOP], which might compensate for their smaller size and lead to a slower

diffusion.

When dissolving the gases, the self-diffusion coefficients of the ions stay the same or slightly increase. There is no evidence of strong relation of the diffusion coefficients depending on either gas or water content (for the amounts tested). If the gases had a strong interaction with the ionic liquids studied, it would be expected that the gases would have a drag effect, decreasing the self-diffusion coefficients. We can safely conclude that the gases had only a diluting effect in the ionic liquids, increasing the spacing between the ion pairs, and decreasing the mixtures' viscosity, leading to an increased flow and self-diffusion coefficients. This is in agreement with the thermodynamic properties of solvation discussed above that do not point towards a dissolution determined by favourable gas-ionic liquid interactions.

Table 3: Self-diffusion coefficients, represented in different forms, D_{log} in $log(m^2/s)$ or D in $10^{-12}(m^2/s)$, of the cation in the ionic liquids in the absence (D) and presence of ethane (D ethane) at different water contents (w/ppm) and corresponding viscosities ($\eta/mPa \cdot s$)

	w	η	D_{log}	D_{log} ethane	D	D ethane
	8396.8		-11.59	-11.58	2.6	2.6
[C$_4$C$_1$Im][DMP]	741.8		-11.72	-11.70	1.9	2.0
	100 - 150	774				
	1020.3		-11.62	-11.58	2.4	2.6
[P$_{6,6,6,14}$][DiOP]	287.4		-11.86	-11.48	1.4	3.3
	100 - 150	1346				

Table 4: Self-diffusion coefficients, represented in different forms, D_{log} in $log(m^2/s)$ or D in $10^{-12}(m^2/s)$, of the cation in the ionic liquids in the absence (D) and presence of ethylene (D ethylene) at different water contents (w/ppm) and corresponding viscosities ($\eta/mPa \cdot s$)

	w	η	D_{log}	D_{log} ethylene	D	D ethylene
	8396.8		-11.59	-11.29	2.6	5.1
[C$_4$C$_1$Im][DMP]	741.8		-11.72	-11.69	1.9	2.0
	100 - 150	774				
	1020.3		-11.62	-10.76	2.4	17
[P$_{6,6,6,14}$][DiOP]	287.4		-11.85	-11.45	1.4	3.5
	100 - 150	1346				

Table 5: Self-diffusion coefficients, represented in different forms, D_{log} in $\log(m^2/s)$ or D in $10^{-12}(m^2/s)$, of the cation in the ionic liquids in the absence (D) and presence of propylene (D propylene) at different water contents (w/ppm) and corresponding viscosities ($\eta/mPa \cdot s$)

	w	η	D_{log}	D_{log} propylene	D	D propylene
	8396.8		-11.58	-11.42	2.6	3.8
$[C_4C_1Im][DMP]$	741.8		-11.56	-11.58	2.8	2.7
	100 - 150	774				
	1020.3		-11.29	-11.71	5.1	1.9
$[P_{6,6,6,14}][DiOP]$	287.4		-11.48	-11.54	3.3	2.9
	100 - 150	1346				

Previous studies have demonstrated that the knowledge of the self-diffusion coefficients can help to establish and quantify the degree of interactions between a solute and an ionic liquid solvent. This was done by D'Agostino *et al.* who determined the self-diffusion coefficients of neat 1-ethyl-3-methylimidazolium acetate, $[C_2C_1Im][OAc]$, and compared it with the self-diffusion coefficients of its mixtures with glucose.[47] The authors found that the self-diffusion coefficient for the cation and anion decreased upon the addition of glucose, for the cation from 12.8 to 3.9 $10^{-11}m^2/s$, and for the anion from 12.5 to 3.1 $10^{-11}m^2/s$. These results are compatible with considering that glucose acts as a disrupting agent in the ionic liquid, the anion forming hydrogen bonds with the sugar's hydroxyl groups.

Conclusions

The solubility of ethane, ethylene, propane and propylene in $[C_4C_1Im][DMP]$ and $[P_{6,6,6,14}][DiOP]$ was precisely measured and the corresponding enthalpy and entropy of solvation were calculated and analysed. From these results, it was possible to evaluate the relative importance of the cohesive energy of the solvent and the gas-ionic liquid interactions in the choice of the ionic liquids that can selectively separate gaseous alkane/alkene mixtures.

The results herein show that $[C_4C_1Im][DMP]$ has lower capacity to absorb the studied gases than $[P_{6,6,6,14}][DiOP]$. The thermodynamic properties of solvation revealed that, in

all studied cases, the gas solvation is entropically driven. $[P_{6,6,6,14}][DiOP]$ shows a more favourable entropy of solvation, a lower density, a lower energy barrier to shear stress and faster ion diffusivities. These properties suggest a "looser" ion packing in $[P_{6,6,6,14}][DiOP]$ when compared with $[C_4C_1Im][DMP]$, a microscopic structure usually more favourable to accommodate the gases.

The solubility results, along with 2D NMR studies, confirm that the gas solubilities in $[C_4C_1Im][DMP]$ and $[P_{6,6,6,14}][DiOP]$ are ruled by non-specific gas-ionic liquid interactions. The results point towards solvation taking place preferentially in the non-polar domains of the ionic liquids, which is compatible with some degree microscopic restructuring, as previously reported by other research groups.[68] These finding point to the fact that the cohesive energy density and flexibility of the ions that form the ionic liquids cannot be overlooked in the rational design of effective absorbents for olefin/paraffin separation.

Acknowledgement

References

(1) Eldridge, R. B. Olefin/paraffin separation technology: a review. *Industrial & engineering chemistry research* **1993**, *32*, 2208–2212.

(2) Sholl, D. S.; Lively, R. P. Seven chemical separations to change the world. *Nature News* **2016**, *532*, 435–437.

(3) Huang, W.; McCormick, J. R.; Lobo, R. F.; Chen, J. G. Selective hydrogenation of acetylene in the presence of ethylene on zeolite-supported bimetallic catalysts. *Journal of Catalysis* **2007**, *246*, 40–51.

(4) Bachman, J. E.; Smith, Z. P.; Li, T.; Xu, T.; Long, J. R. Enhanced ethylene separation and plasticization resistance in polymer membranes incorporating metal–organic framework nanocrystals. *Nature materials* **2016**, *15*, 845–849.

(5) Lu, C.; Chen, Y.; Wang, Y.; Du, Y.; Yang, J.; Li, L.; Li, J. Energy efficient ethylene purification in a commercially viable ethane-selective MOF. *Separation and Purification Technology* **2022**, *282*, 120126.

(6) Chuah, C. Y.; Lee, H.; Bae, T.-H. Recent advances of nanoporous adsorbents for light hydrocarbon (C1–C3) separation. *Chemical Engineering Journal* **2022**, *430*, 132654.

(7) Su, K.; Wang, W.; Du, S.; Ji, C.; Yuan, D. Efficient ethylene purification by a robust ethane-trapping porous organic cage. *Nature Communications* **2021**, *12*, 1–7.

(8) Yang, Y.; Li, L.; Lin, R.-B.; Ye, Y.; Yao, Z.; Yang, L.; Xiang, F.; Chen, S.; Zhang, Z.; Xiang, S., et al. Ethylene/ethane separation in a stable hydrogen-bonded organic framework through a gating mechanism. *Nature Chemistry* **2021**, *13*, 933–939.

(9) Cui, X.; Chen, K.; Xing, H.; Yang, Q.; Krishna, R.; Bao, Z.; Wu, H.; Zhou, W.; Dong, X.; Han, Y., et al. Pore chemistry and size control in hybrid porous materials for acetylene capture from ethylene. *Science* **2016**, *353*, 141–144.

(10) Wang, Y.; Ghanem, B. S.; Han, Y.; Pinnau, I. State-of-the-art polymers of intrinsic microporosity for high-performance gas separation membranes. *Current Opinion in Chemical Engineering* **2022**, *35*, 100755.

(11) Lai, B.; Cahir, J.; Tsang, M. Y.; Jacquemin, J.; Rooney, D.; Murrer, B.; James, S. L. Type 3 Porous Liquids for the Separation of Ethane and Ethene. *ACS Applied Materials & Interfaces* **2020**, *13*, 932–936.

(12) Xu, Y.; Xu, J.; Yang, C. Molecule design of effective C2H4/C2H6 separation membranes: From 2D nanoporous graphene to 3D AHT zeolite. *Journal of Membrane Science* **2020**, *604*, 118033.

(13) Ren, Y.; Liang, X.; Dou, H.; Ye, C.; Guo, Z.; Wang, J.; Pan, Y.; Wu, H.; Guiver, M. D.; Jiang, Z. Membrane-Based Olefin/Paraffin Separations. *Advanced Science* **2020**, *7*, 2001398.

(14) Dou, H.; Jiang, B.; Xu, M.; Zhou, J.; Sun, Y.; Zhang, L. Supported ionic liquid membranes with high carrier efficiency via strong hydrogen-bond basicity for the sustainable and effective olefin/paraffin separation. *Chemical Engineering Science* **2019**, *193*, 27–37.

(15) Dou, H.; Jiang, B.; Zhang, L.; Xu, M.; Sun, Y. Synergy of high permeability, selectivity and good stability properties of silver-decorated deep eutectic solvent based facilitated transport membranes for efficient ethylene/ethane separation. *Journal of Membrane Science* **2018**, *567*, 39–48.

(16) Yang, K.; Ban, Y.; Yang, W. Layered MOF membranes modified with ionic liquid/AgBF4 composite for olefin/paraffin separation. *Journal of Membrane Science* **2021**, *639*, 119771.

(17) Campos, A. C. C.; dos Reis, R. A.; Ortiz, A.; Gorri, D.; Ortiz, I. A perspective of solutions for membrane instabilities in olefin/paraffin separations: a review. *Industrial & Engineering Chemistry Research* **2018**, *57*, 10071–10085.

(18) Safarik, D. J.; Eldridge, R. B. Olefin/paraffin separations by reactive absorption: a review. *Industrial & engineering chemistry research* **1998**, *37*, 2571–2581.

(19) de Haan, A. B.; Eral, H. B.; Schuur, B. *Industrial separation processes:fundamentals*; De Gruyter: Berlin, Boston, **2020**.

(20) Moura, L.; Santini, C. C.; Gomes, M. F. C. Gaseous hydrocarbon separations using functionalized ionic liquids. *Oil & Gas Science and Technology–Revue d'IFP Energies nouvelles* **2016**, *71*, 23.

(21) Huang, Y.; Zhang, Y.; Xing, H. Separation of light hydrocarbons with ionic liquids: A review. *Chinese Journal of Chemical Engineering* **2019**, *27*, 1374–1382.

(22) Shiflett, M. B. *Commercial applications of ionic liquids*; Springer, **2020**; Vol. 605.

(23) Liu, X.; Afzal, W.; Prausnitz, J. M. Solubilities of Small Hydrocarbons in Tetra-butylphosphonium Bis (2, 4, 4-trimethylpentyl) Phosphinate and in 1-Ethyl-3-methylimidazolium Bis (trifluoromethylsulfonyl) imide. *Industrial & Engineering Chemistry Research* **2013**, *52*, 14975–14978.

(24) Liu, X.; Afzal, W.; Yu, G.; He, M.; Prausnitz, J. M. High solubilities of small hydro-carbons in trihexyl tetradecylphosphonium bis (2, 4, 4-trimethylpentyl) phosphinate. *The Journal of Physical Chemistry B* **2013**, *117*, 10534–10539.

(25) Moura, L.; Mishra, M.; Bernales, V.; Fuentealba, P.; Padua, A. A.; Santini, C. C.; Costa Gomes, M. F. Effect of Unsaturation on the Absorption of Ethane and Ethylene in Imidazolium-Based Ionic Liquids. *The Journal of Physical Chemistry B* **2013**, *117*, 7416–7425.

(26) Zhao, X.; Yang, Q.; Xu, D.; Bao, Z.; Zhang, Y.; Su, B.; Ren, Q.; Xing, H. Design and screening of ionic liquids for C2H2/C2H4 separation by COSMO-RS and experiments. *AIChE Journal* **2015**, *61*, 2016–2027.

(27) Banerjee, T.; Khanna, A. Infinite dilution activity coefficients for trihexyltetradecyl

phosphonium ionic liquids: measurements and COSMO-RS prediction. *Journal of Chemical & Engineering Data* **2006**, *51*, 2170–2177.

(28) Ferguson, L.; Scovazzo, P. Solubility, diffusivity, and permeability of gases in phosphonium-based room temperature ionic liquids: data and correlations. *Industrial & engineering chemistry research* **2007**, *46*, 1369–1374.

(29) Xing, H.; Zhao, X.; Li, R.; Yang, Q.; Su, B.; Bao, Z.; Yang, Y.; Ren, Q. Improved efficiency of ethylene/ethane separation using a symmetrical dual nitrile-functionalized ionic liquid. *ACS Sustainable Chemistry & Engineering* **2013**, *1*, 1357–1363.

(30) Moura, L.; Darwich, W.; Santini, C. C.; Gomes, M. F. C. Imidazolium-based ionic liquids with cyano groups for the selective absorption of ethane and ethylene. *Chemical Engineering Journal* **2015**, *280*, 755–762.

(31) Liu, X.; Liu, S.; Bai, L.; Wang, T.; He, M. Absorption and separation of CO2/C3H8 and C3H6/C3H8 by ionic liquid: Effect of molar volume. *Journal of Natural Gas Science and Engineering* **2018**, *58*, 266–274.

(32) Makino, T.; Kanakubo, M. Absorption of n-butane in imidazolium and phosphonium ionic liquids and application to separation of hydrocarbon gases. *Separation and Purification Technology* **2019**, *214*, 139–147.

(33) Xu, G.; Shi, M.; Zhang, P.; Tu, Z.; Hu, X.; Zhang, X.; Wu, Y. Tuning the composition of deep eutectic solvents consisting of tetrabutylammonium chloride and n-decanoic acid for adjustable separation of ethylene and ethane. *Separation and Purification Technology* **2022**, 121680.

(34) Martins, M. A. R.; Pinho, S. P.; Coutinho, J. A. P. Insights into the Nature of Eutectic and Deep Eutectic Mixtures. *Journal of Solution Chemistry* **2019**, *48*, 962–982.

(35) Xu, M.; Jiang, B.; Dou, H.; Yang, N.; Xiao, X.; Tantai, X.; Sun, Y.; Zhang, L. Double-salt ionic liquid derived facilitated transport membranes for ethylene/ethane separation. *Journal of Membrane Science* **2021**, *639*, 119773.

(36) Sanchez, C. M.; Song, T.; Brennecke, J. F.; Freeman, B. D. Hydrogen stable supported ionic liquid membranes with silver carriers: propylene and propane permeability and solubility. *Industrial & Engineering Chemistry Research* **2019**, *59*, 5362–5370.

(37) Park, S.; Morales-Collazo, O.; Freeman, B.; Brennecke, J. F. Ionic Liquid Stabilizes Olefin Facilitated Transport Membranes Against Reduction. *Angewandte Chemie International Edition* **2022**, e202202895.

(38) Liang, X.; Wu, H.; Huang, H.; Wang, X.; Wang, M.; Dou, H.; He, G.; Ren, Y.; Liu, Y.; Wu, Y., et al. Efficient ethylene/ethane separation through ionic liquid-confined covalent organic framework membranes. *Journal of Materials Chemistry A* **2022**, *10*, 5420–5429.

(39) Dou, H.; Jiang, B.; Xu, M.; Zhang, Z.; Wen, G.; Peng, F.; Yu, A.; Bai, Z.; Sun, Y.; Zhang, L., et al. Boron nitride membranes with a distinct nanoconfinement effect for efficient ethylene/ethane separation. *Angewandte Chemie* **2019**, *131*, 14107–14113.

(40) Sun, J.; Howlett, P. C.; MacFarlane, D. R.; Lin, J.; Forsyth, M. Synthesis and physical property characterisation of phosphonium ionic liquids based on P(O)2(OR)2- and P(O)2(R)2- anions with potential application for corrosion mitigation of magnesium alloys. *Electrochimica Acta* **2008**, *54*, 254–260.

(41) Kuhlmann, E.; Himmler, S.; Giebelhaus, H.; Wasserscheid, P. Imidazolium dialkylphosphates—a class of versatile, halogen-free and hydrolytically stable ionic liquids. *Green Chem.* **2007**, *9*, 233–242.

(42) Jacquemin, J.; Husson, P.; Majer, V.; Costa Gomes, M. Low-Pressure Solubilities and

Thermodynamics of Solvation of Eight Gases in 1-Butyl-3-Methylimidazolium Hexafluorophosphate. *Fluid Phase Equilibria* **2006**, *240*, 87–95.

(43) Costa Gomes, M. F. Low-Pressure Solubility and Thermodynamics of Solvation of Carbon Dioxide, Ethane, and Hydrogen in 1-Hexyl-3-Methylimidazolium Bis(Trifluoromethylsulfonyl)Amide between Temperatures of 283 K and 343 K. *Journal of Chemical & Engineering Data* **2007**, *52*, 472–475.

(44) Dymond, J.; Marsh, K.; Wilhoit, R.; Wong, K. *Virial Coefficients of Pure Gases and Mixtures - Subvolume A: Virial Coefficients of Pure Gases*; Springer-Verlag Berlin Heidelberg: Berlin, Germany, **2002**.

(45) Avila, J.; Červinka, C.; Dugas, P.-Y.; Pádua, A. A. H.; Costa Gomes, M. Porous Ionic Liquids: Structure, Stability, and Gas Absorption Mechanisms. *Advanced Materials Interfaces* **2021**, *8*, 2001982.

(46) Zanatta, M.; Antunes, V. U.; Tormena, C. F.; Dupont, J.; Dos Santos, F. P. Dealing with supramolecular structure for ionic liquids: a DOSY NMR approach. *Physical Chemistry Chemical Physics* **2019**, *21*, 2567–2571.

(47) D'Agostino, C.; Mantle, M. D.; Mullan, C. L.; Hardacre, C.; Gladden, L. F. Diffusion, Ion Pairing and Aggregation in 1-Ethyl-3-Methylimidazolium-Based Ionic Liquids Studied by 1H and 19F PFG NMR: Effect of Temperature, Anion and Glucose Dissolution. *ChemPhysChem* **2018**, *19*, 1081–1088.

(48) Maton, C.; De Vos, N.; Stevens, C. V. Ionic liquid thermal stabilities: decomposition mechanisms and analysis tools. *Chemical Society Reviews* **2013**, *42*, 5963–5977.

(49) Clough, M. T.; Crick, C. R.; Gräsvik, J.; Hunt, P. A.; Niedermeyer, H.; Welton, T.; Whitaker, O. P. A physicochemical investigation of ionic liquid mixtures. *Chemical science* **2015**, *6*, 1101–1114.

(50) Brandt, A.; Hallett, J. P.; Leak, D. J.; Murphy, R. J.; Welton, T. The effect of the ionic liquid anion in the pretreatment of pine wood chips. *Green Chemistry* **2010**, *12*, 672–679.

(51) Silva, A. A.; Livi, S.; Netto, D. B.; Soares, B. G.; Duchet, J.; Gérard, J.-F. New epoxy systems based on ionic liquid. *Polymer* **2013**, *54*, 2123–2129.

(52) Yu, B.; Bansal, D. G.; Qu, J.; Sun, X.; Luo, H.; Dai, S.; Blau, P. J.; Bunting, B. G.; Mordukhovich, G.; Smolenski, D. J. Oil-miscible and non-corrosive phosphonium-based ionic liquids as candidate lubricant additives. *Wear* **2012**, *289*, 58–64.

(53) Xue, Z.; Qin, L.; Jiang, J.; Mu, T.; Gao, G. Thermal, electrochemical and radiolytic stabilities of ionic liquids. *Physical Chemistry Chemical Physics* **2018**, *20*, 8382–8402.

(54) Wang, B.; Qin, L.; Mu, T.; Xue, Z.; Gao, G. Are ionic liquids chemically stable? *Chemical reviews* **2017**, *117*, 7113–7131.

(55) Del Sesto, R. E.; Corley, C.; Robertson, A.; Wilkes, J. S. Tetraalkylphosphonium-based ionic liquids. *Journal of Organometallic Chemistry* **2005**, *690*, 2536–2542.

(56) Lovelock, K. R. J. Quantifying intermolecular interactions of ionic liquids using cohesive energy densities. *Royal Society Open Science* **2017**, *4*, 171223.

(57) Santos, L. M. N. B. F.; Canongia Lopes, J. N.; Coutinho, J. A. P.; Esperança, J. M. S. S.; Gomes, L. R.; Marrucho, I. M.; Rebelo, L. P. N. Ionic Liquids: First Direct Determination of their Cohesive Energy. *Journal of the American Chemical Society* **2007**, *129*, 284–285.

(58) Kestin, J.; Sokolov, M.; Wakeham, W. A. Viscosity of liquid water in the range -8°C to 150°C. *Journal of Physical and Chemical Reference Data* **1978**, *7*, 941–948.

(59) van den Bruinhorst, A. Deep eutectic solvents : a new generation of designer solvents. Ph.D. thesis, Technische Universiteit Eindhoven, **2018**.

(60) Liu, X.; Afzal, W.; Yu, G.; He, M.; Prausnitz, J. M. High Solubilities of Small Hydrocarbons in Trihexyl Tetradecylphosphonium Bis(2,4,4-trimethylpentyl) Phosphinate. *The Journal of Physical Chemistry B* **2013**, *117*, 10534–10539.

(61) Stassen, H. K.; Ludwig, R.; Wulf, A.; Dupont, J. Imidazolium Salt Ion Pairs in Solution. *Chemistry – A European Journal* **2015**, *21*, 8324–8335.

(62) Otto, S. The role of solvent cohesion in nonpolar solvation. *Chemical Science* **2013**, *4*, 2953–2959.

(63) Marcus, Y. Internal Pressure of Liquids and Solutions. *Chemical Reviews* **2013**, *113*, 6536–6551.

(64) Fulmer, G. R.; Miller, A. J.; Sherden, N. H.; Gottlieb, H. E.; Nudelman, A.; Stoltz, B. M.; Bercaw, J. E.; Goldberg, K. I. NMR chemical shifts of trace impurities: common laboratory solvents, organics, and gases in deuterated solvents relevant to the organometallic chemist. *Organometallics* **2010**, *29*, 2176–2179.

(65) Tokuda, H.; Hayamizu, K.; Ishii, K.; Susan, M. A. B. H.; Watanabe, M. Physicochemical Properties and Structures of Room Temperature Ionic Liquids. 1. Variation of Anionic Species. *The Journal of Physical Chemistry B* **2004**, *108*, 16593–16600.

(66) Tokuda, H.; Hayamizu, K.; Ishii, K.; Susan, M. A. B. H.; Watanabe, M. Physicochemical Properties and Structures of Room Temperature Ionic Liquids. 2. Variation of Alkyl Chain Length in Imidazolium Cation. *The Journal of Physical Chemistry B* **2005**, *109*, 6103–6110.

(67) Tokuda, H.; Ishii, K.; Susan, M. A. B. H.; Tsuzuki, S.; Hayamizu, K.; Watanabe, M. Physicochemical Properties and Structures of Room-Temperature Ionic Liquids. 3. Variation of Cationic Structures. *The Journal of Physical Chemistry B* **2006**, *110*, 2833–2839.

(68) Corvo, M. C.; Sardinha, J.; Menezes, S. C.; Einloft, S.; Seferin, M.; Dupont, J.; Casimiro, T.; Cabrita, E. J. Solvation of Carbon Dioxide in [C4mim][BF4] and [C4mim][PF6] Ionic Liquids Revealed by High-Pressure NMR Spectroscopy. *Angewandte Chemie International Edition* **2013**, *52*, 13024–13027.